IEEE Access
Multidisciplinary | Rapid Review | Open Access Journal

Received March 30, 2022, accepted April 7, 2022, date of publication April 14, 2022, date of current version April 27, 2022.

Digital Object Identifier 10.1109/ACCESS.2022.3167387

Compact Super Wideband Frequency Diversity Hexagonal Shaped Monopole Antenna With Switchable Rejection Band

YANAL FAOURI[1], (Senior Member, IEEE), SAROSH AHMAD[2,3], (Student Member, IEEE), SALMAN NASEER[4], KHALID ALHAMMAMI[1], (Member, IEEE), NOOR AWAD[1], ADNAN GHAFFAR[5], AND MOUSA I. HUSSEIN[6], (Senior Member, IEEE)

[1]Department of Electrical Engineering, The University of Jordan, Amman 11942, Jordan
[2]Department of Electrical Engineering and Technology, Government College University Faisalabad (GCUF), Faisalabad 38000, Pakistan
[3]Department of Signal Theory and Communications, Universidad Carlos III de Madrid, Leganés, 28911 Madrid, Spain
[4]Department of Information Technology, University of the Punjab, Gujranwala Campus, Gujranwala 52250, Pakistan
[5]Department of Electrical and Electronic Engineering, Auckland University of Technology, Auckland 1010, New Zealand
[6]Department of Electrical Engineering, United Arab Emirates University, Al Ain, United Arab Emirates

Corresponding authors: Sarosh Ahmad (saroshahmad@ieee.org) and Mousa I. Hussein (mihussein@uaeu.ac.ae)

ABSTRACT To reduce interference from other wireless communications, a compact super wideband frequency diversity hexagonal shaped monopole antenna with switchable rejection band capabilities is proposed. The patch consists of hexagonal structure with an open-ended horizontal slot that divides the patch into upper and lower parts. The overall size of the proposed antenna is 36 mm × 36 mm × 1.6 mm on an FR-4 substrate material with a loss tangent of $tan\delta = 0.02$. The notch switchable features and the frequency diversity are controlled by changing the length of the resonator through alternating the state of two inserted parallel PIN diodes inside the horizontal open-ended slot. The upper part of the hexagonal patch is connected to the negative terminal of the diodes and the biasing circuit in the back layer through a conducting via. The lower part is connected to the positive terminal of the diode. When both diodes are OFF, the proposed antenna behaves as a super wideband covering a bandwidth from 3.37 GHz to 27.71 GHz. When both diodes are ON, there is a band notch and a frequency a frequency band (3.81 - 6.62 GHz) is filtered. The antenna's radiation pattern is broadsided directional, and the efficiency is observed 92.9% and 96% for the ON and OFF cases, respectively. The reflection coefficient (S_{11}) at the rejection band is −3.06 dB at 5.38 GHz. Hence, the proposed super wideband antenna is well-suited for applications in wireless communications.

INDEX TERMS Super wideband, frequency reconfigurable, notch characteristics, PIN diodes, time-domain analysis.

I. INTRODUCTION

Since the establishment of the unlicensed Ultra-Wide Band (UWB) band of 3.1 - 10.6 GHz for Ultra-Wide Band communications in 2002 [1], a considerable number of studies have begun to embed super wideband (SWB) technology into wireless communication devices to satisfy the need for both long and short distance communication. Many super wideband (SWB) monopole antennas research are offered to focus on bandwidth improvement techniques used in the ground plane, feed line, and the radiating patch. Different techniques to offer SWB are discussed in [2], these techniques include modifications to the patch and ground plane shapes besides adding different slot shapes or stubs in different antenna locations. In [3], the antenna was designed to cover a wide frequency range of 1.22 to 47.5 GHz by having a concentric structured monopole patch shape and semi-elliptic ground plane with one notch at its top. A microstrip antenna had a shape of fractal hexagonal Sierpinski was described in [4] realized an impedance bandwidth of 3.4 - 37.4 GHz. A stub on the top right corner of an octagonal ring patch and a notch on the ground plane increases the impedance bandwidth to span the frequency range of 2.59 to 31.14 GHz [5]. Two ground planes on the top side and a partial ground

The associate editor coordinating the review of this manuscript and approving it for publication was Kwok L. Chung.

plane on the bottom side were used in [6] to offer bandwidth in the band of 0.3-20 GHz.

Several antennas that exhibit a hexagonal shape have been reported for super wideband coverage. In [7], a 31 mm × 45 mm × 1.575 mm SWB antenna, consists of a fractal circular patch with six iterations of a hexagonal slot inside it to achieve an impedance bandwidth of 2.18 to 44.5 GHz. In [8], an antenna with 36 mm×30 mm×1.6 mm hexagonal patch antenna with two rectangular slots in the ground plane offers a bandwidth between 2.9 GHz to 14.75 GHz. Three iterations of a hexagonal patch containing circular and triangular elements are used in [9] with an antenna size of 25 mm × 30 mm × 0.8 mm to produce a bandwidth starting at 3.5 GHz to 33.5 GHz at $|S_{11}| \leq 10$ dB. In [10], the fractal nature of hexagonal rings and triangular elements are used to produce an antenna that covers a frequency range of 3 - 25.2 GHz.

Other extensively deployed systems such as WLAN and WiMAX cause interference to SWB communication networks, so a demand to design an SWB antenna that can reject these specific bands. A hexagonal patch enclosed by a hexagonal slot is etched in a 25 mm × 25 mm × 1.6 mm antenna to create a notch in the band 5.83 GHz - 6.05 GHz [11]. Two layers of hexagonal patch antenna (SMHPA) that operate in the range of 2-6 GHz are used as slots to create three-band notches centered at 2.8, 3.98, and 5.78 GHz [12]. Employ complementary split-ring resonators CSRR and complementary spiral resonators CSR to provide one notched band for WLAN (5-6) GHz [13]. One stopband at 5.5 GHz is achieved by two L-shaped resonators linked to the ground plane with two shorting tracks on the sides of the antenna [14]. Introducing two equal slots introduced a patch creating one single rejection at 3.75 - 4.875 GHz [15]. A meandered bowtie antenna having six rejecting bands and seven operating bands has been reported in [16] for modern 5G communications by connecting the left bowtie portion to the ground plane via a shorting pin.

Nowadays communications have an urgent need to reconfigure some characteristics in the antenna to meet several demands. Reconfigurable antennas have four types, frequency, polarization, pattern, and bandwidth, or combining two or more reconfigurable aspects in one design. Antennas that change their resonance frequency are known as frequency reconfigurable antennas. PIN diodes, varactors, and MEMs switches are electronic ways that are used to establish a reconfigurability process. PIN diodes are commonly used because of their rapid switching speed, dependability, low biasing voltage required, little current values while switching, and being small. PIN diodes are used to filter certain frequency bands with frequency diversity according to the ON-OFF state [15]. In [17], a circular patch antenna with a PIN diode and a varactor was used to tune the notch central frequency from 4.2 GHz when PIN diodes are ON to 5.8GHz when it is OFF. A UWB antenna is designed with three PIN diodes placed at the ground plane slot to switch between UWB band 1.86 - 10.89 GHz, two stopbands at 2.7 - 3.5 GHz, and 5.43 - 6.44 GHz, and different three notch frequencies [18].

A square patch with a modified shape has different geometrical slots in the patch and ground plane to create a filtration process for WLAN and WiMAX applications as explained in [19]. By placing two PIN diodes in the slots, frequency shift occurs in switching between UWB band that covers 3.1 - 12 GHz, creating two different single notches in the desired frequency band either at 3.3 - 3.7 GHz or 4.9 - 6.3 GHz and creating two notches at 3.3 - 3.7 and 5.1 - 6.5 GHz. Frequency reconfigurability was described in [20], where a slotted triangular-shaped patch is used with four PIN diodes that are placed at different positions in the rectangular slot in the ground plane. Changing the ON-OFF state of the four PIN diodes will create two, three, or four notch frequencies in the 4 - 15 GHz frequency range and change their locations. The author in [21] suggested two PIN diodes in the inverted U slot on the patch and keeping the varactor to a certain place anywhere along the slot will tune the notch frequency in the range 2.7 - 7.2 GHz.

The authors in [22], embed one PIN diode in the small size antenna, 8 × 27.5 mm^2, that has a patch like the G-shaped, and he controls its state to switch between UWB frequency band 2.8 - 12.6 GHz when the diode is ON and creating a band filter at 3.5 - 4.95 GHz when the diode is OFF. In ref [23], tuning the center of the notch band is achieved by inserting one PIN diode in the split ring resonator of the S-letter shape patch, where it occurred at 3.25 GHz when the diode is ON and shift to 5.5 GHz in the OFF state. A UWB antenna that operates in the range 3 - 10.6 GHz is proposed in [24], with two PIN diodes are placed in the patch slots to reject the WiMAX 3.3 – 3.7 GHz and 5 - 5.30 GHz WLAN applications according to the diode states. Moreover, after placing the two diodes in the microstrip lines that were etched parallel to the ladder shape slot and adjusting their position had adjusted the current path which affected the location of the notch center frequency in the range 3.3 - 5.5 GHz [25]. In [26], the author designed an antenna with two band notches by etching two folded end U-shaped slots in the patch, besides they had provided a switchable function using two PIN diodes to switch between UWB band 2.7 - 10.7 GHz, creating one notch at 5.5 - 6.15 GHz and two-band notches at 3.2 – 4.2 and 5.5 - 6.15 GHz.

The reconfigurable hexagonal-shaped antenna was also reported in the literature [27]-[28]. In [27], a dual-band complex shape of a hexagonal shape antenna loaded by a complementary split-ring resonator (CSRR) and integrated with a varactor diode has been reported in [27]. The antenna has UWB coverage, and the varactor controls the level of the rejection band without removing it completely. A hexagonal microstrip antenna fed by a microstrip fed with a rectangular cut in the feed to insert a PIN diode has been reported in [28] to achieve dual-band operation. The ON and OFF states of the diode are responsible for shifting the two resonances without controlling the presence and absence of the rejection band.

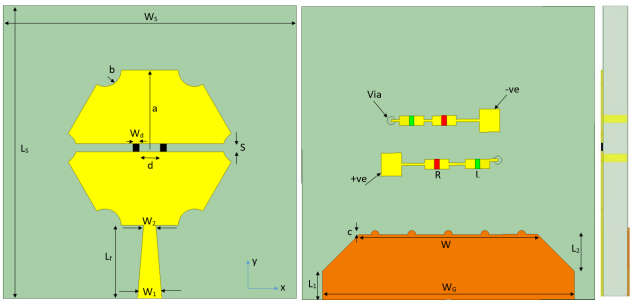

FIGURE 1. Antenna's structure, (a) top layer, (b) baclayer, (c) side view.

TABLE 1. Optimized dimensions of the proposed antenna.

Parameters	Values (mm)	Parameters	Values (mm)
WS	36	LS	36
W1	3	W2	1.5
A	9	B	2
S	1	D	2.5
Lf	9	Wd	0.8
WG	31	W	22
L1	3.5	L2	4.5
c	0.5	Via radius	0.5

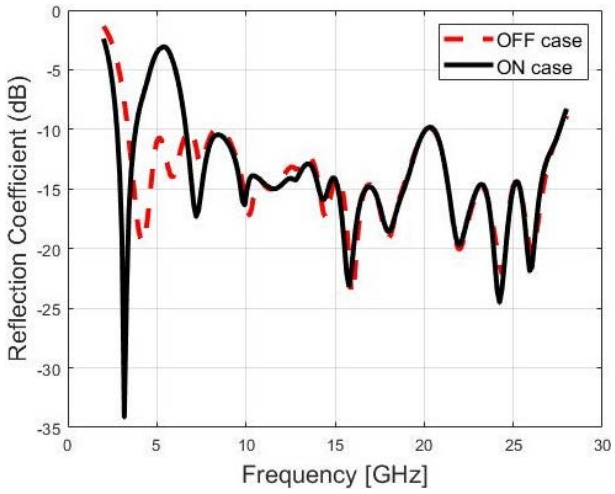

FIGURE 2. S_{11} of the designed antenna for both diodes configurations.

In this article, a small size super wideband (SWB) frequency diversity hexagonal monopole antenna with switchable rejection band capabilities is proposed. The antenna covers a wide band with a percentage bandwidth of 156.6% and a good bandwidth dimension ratio (BDR) reaches 978.8. Furthermore, the antenna can activate or deactivate one wide rejection band by adding two parallel common anode PIN diodes at the patch horizontal open-ended slot and controlling their ON/OFF states. The rejection band is produced when both diodes are in the ON state which lies in the range of

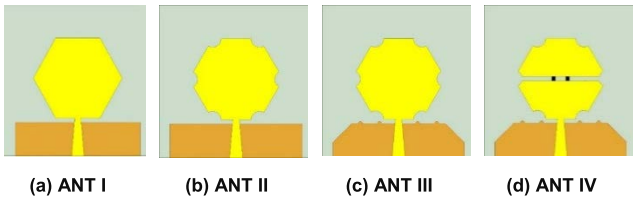

FIGURE 3. Proposed antenna design steps: (a) Hexagonal patch with the partial ground (ANT I), (b) Modified hexagonal patch with the partial grounIANT II), (c) Modified patch with the enhanced ground (ANT III), and (d) Proposed design (ANT IV).

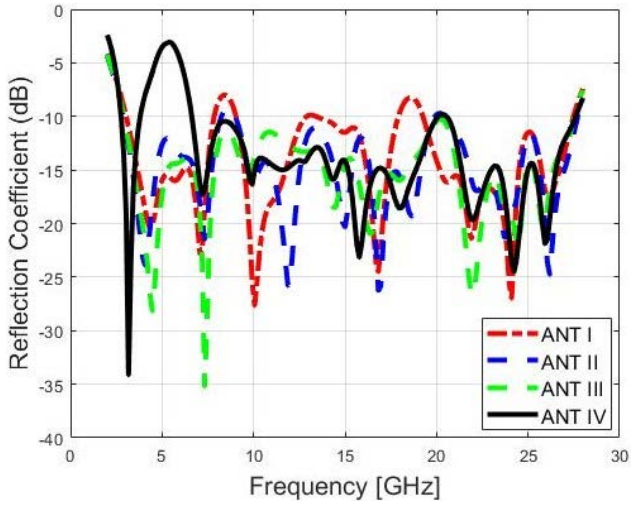

FIGURE 4. S_{11} of the four designed antenna steps presented in Figure 3.

3.5 GHz to 4.95 GHz with the S_{11} level at the center of the rejection band reaches to −4.34 dB. The antenna ON/OFF states are modelled in an equivalent circuit by investigating the parametric effect of their components. Also, the designed antenna operation has been investigated in the time domain. The analysis of the design of the frequency reconfigurable antenna is outlined in Section 2. Proposed antenna analysis and equivalent circuit model are illustrated in Section 3, experimental validation is outlined in Section 4, and the conclusion is presented in Section 5.

II. ANTENNA DESIGN ANALYSIS

A. ANTENNA STRUCTURE

The suggested patch antenna schematic diagram for the top, back, and side views are shown in Figure 1. The simulations and optimizations have been supported by high-frequency structure simulator (HFSS) software. The antenna was built using a low-cost substrate known as FR-4 (relative permittivity of 4.4, loss tangent of 0.02) that has an overall size of 36 × 36 × 1.6 mm^3. The patch has a hexagonal shape with curved corners and is fed by a tapered feedline for better impedance matching between the 50-Ω coaxial cable connected to the SMA connector and the high impedance at the patch edge. A horizontal slot in the patch center with a width of 1 mm is introduced to insert two parallel common anode PIN diodes with a footprint of 1 mm x 0.8 mm

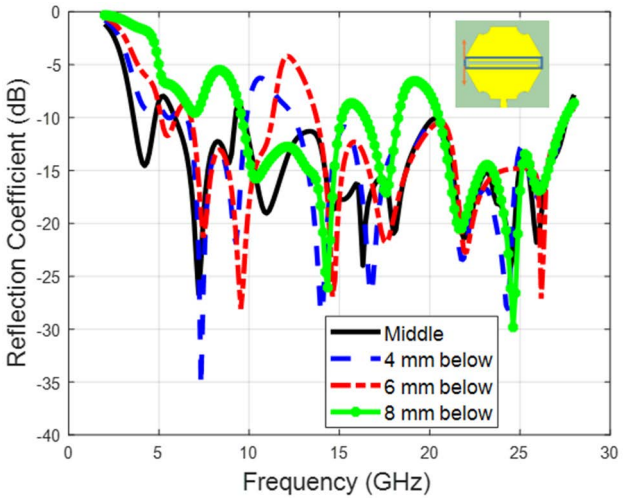

FIGURE 5. S_{11} variations for various slot locations.

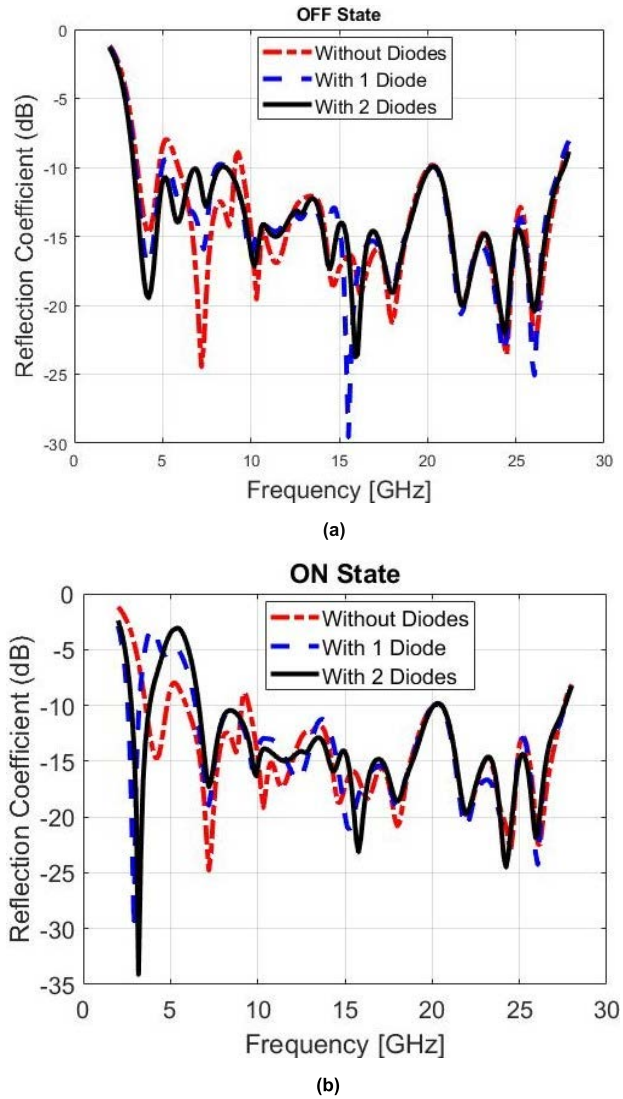

FIGURE 6. The effect of adding the PIN diodes on the reflection coefficient for (a) OFF case, and (b) ON case.

being placed at the center of the horizontal slot for frequency diversity analysis. The diodes are connected via shorting vias

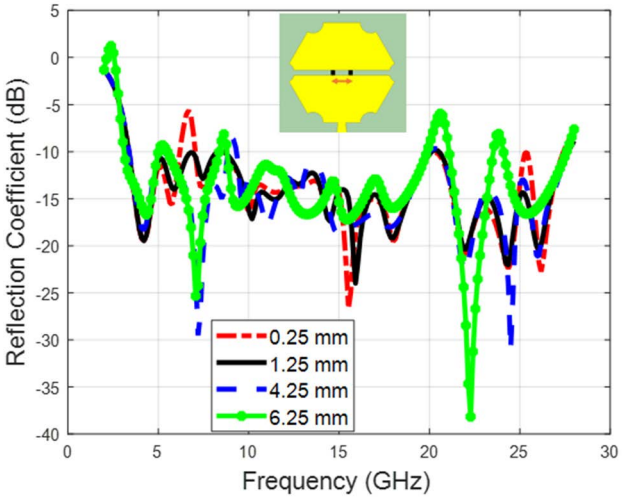

FIGURE 7. S_{11} variations for various diodes separations.

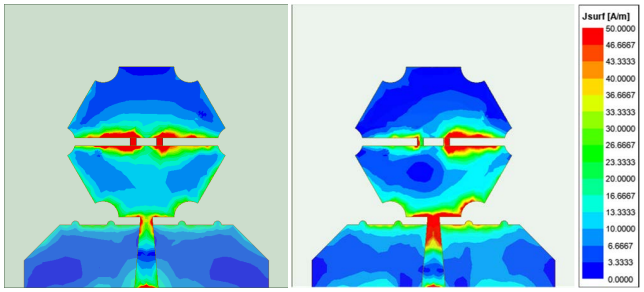

FIGURE 8. Surface current distribution (a) at 3.17 GHz and (b) at 5.38 GHz.

to a separate DC biasing circuit placed at the bottom layer as shown in Figure 1I and both diodes are activated and deactivated simultaneously since they relate to the common anode and common cathode configuration. The biasing line is connected to a 2 – 5 V supply and passes through a 2.1 kΩ for current limiting and a 1 μH inductor to act as an open circuit to the RF signal and a short circuit for the DC biasing. The proposed antenna ground plane has a trapezoidal shape with five circular sleeves. Extensive parametric analysis has been conducted on all the parameters and their optimized values are recorded in Table 1.

The proposed antenna reflection coefficient (S_{11}) is plotted in Figure 2 for both dio'es' status. When the diodes are in the OFF state, the antenna covers an SWB of 3.37 – 27.71 GHz without any rejection bands while in the ON state a notch will be created at 5.38 GHz with a frequency range of 3.81 – 6.62 GHz, making the antenna has dual bands 2.76 – 5.81 GHz and 6.62 – 27.61 GHz with a percentage bandwidth (PBW) of 31.96 % and 122.64 % respectively with a 10:1 bandwidth ratio.

B. ANTENNA DESIGN STEPS

The antenna design steps are shown in Figure 3 and the simulated S_{11} results for all steps are shown in Figure 4. ANT I consists of a simple hexagonal patch, partial ground

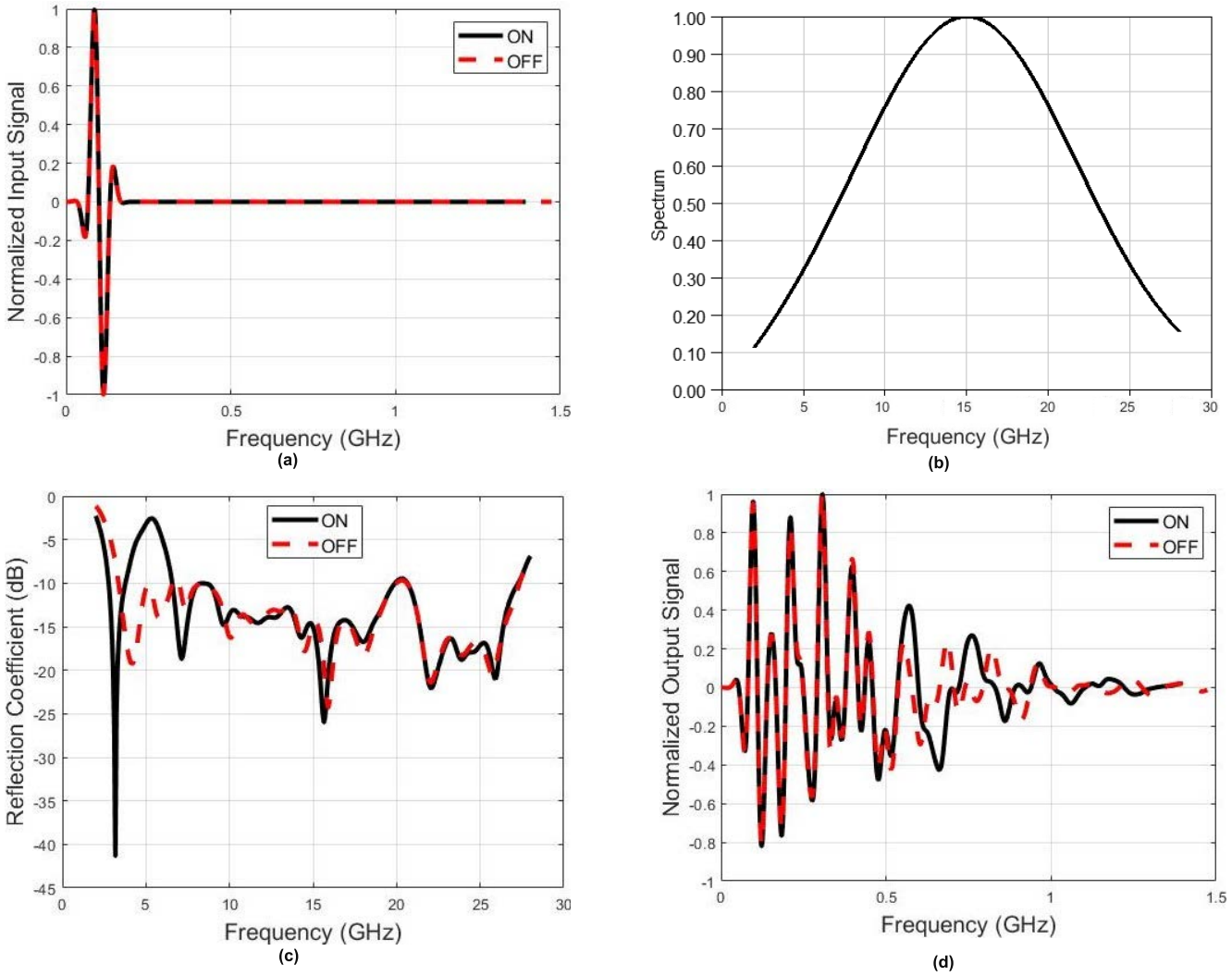

FIGURE 9. Time-domain results of the proposed ana showing (a) (a) Input pulse, (b) input spectrum, (c) Fourier transform of the input signal, and (d) output signals.

plane, and 50 Ω triangular tapered feedline. The hexagonal shape was chosen because the bandwidth of a circular patch antenna is higher than any other geometry, and the hexagonal geometry is almost identical to a circular patch. The dimensions of the hexagonal antenna are calculated by adjusting the planar disc formula as explained in [29]. The tapered feed line is a matching transformer between the point of feeding and the hexagonal patch which will provide a smooth impedance transition, reduce the reflection of the incident wave, and enhance the antenna bandwidth [30]. Impedance matching and improved bandwidth were achieved with the help of ANT II and ANT III. In ANT II, after curving the hexagonal patch vertices better impedance matching was achieved while beveling the ground plane in ANT III and adding five half-circular sleeves at the top of it provided wider bandwidth of 2.91 – 27.54 GHz. Beveling the ground plane and adding the sleeves improve the total bandwidth, raise the inductive component of the input impedance, and generate more resonant modes [31]–[33].

The proposed antenna is shown in ANT IV, where an open-ended horizontal slot is inserted at the center of the hexagonal patch which divides it into upper and lower parts to create a space for PIN diodes insertion. The PIN diodes are represented by a 3 Ω resistor when it is at the ON-state and by a 0.2 pF capacitor when it is at the OFF-state [34]. The upper and lower parts of the hexagonal patch are connected to the negative and positive polarities of the (2-5) V external DC biasing circuit respectively through vias between the top and the back of the antenna. The S_{11} response for ANT IV in its OFF state is like ANT III but with the ability to control its frequency characteristics.

C. PARAMETRIC STUDY OF THE PROPOSED ANTENNA

A parametric study of the proposed antenna is oriented to focus on the three main stages, namely, the location of the horizontal slot, the number of diodes used in the slot, and the distance between the diodes as depicted in Figures 5 - 7. First, the horizontal slot has been varied along with the

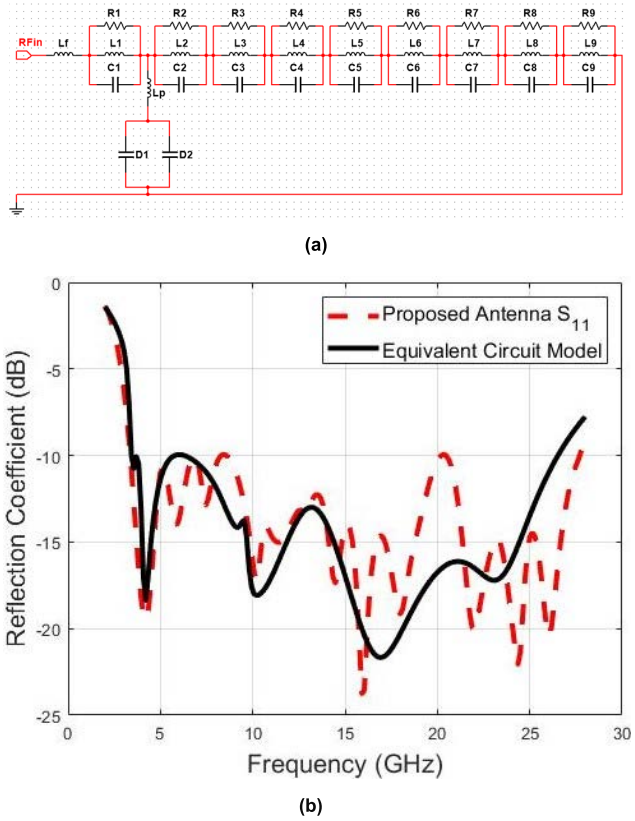

FIGURE 10. (a) Equivalent circuit model and (b) reflection coefficient of the equivalent circuit model when the diodes are in the OFF case.

TABLE 2. Values of the components used in the circuit model for the OFF case R, C (pF), L (pH)).

R1 = 50.61	R2 = 104.8	R3 = 5.866	R4 = 28.141	R5 = 29.873
L1 = 813.24	L2 = 30.564	L3 = 0.058	L4 = 190.29	L5 = 515.23
C1 = 0.385	C2 = 8.767	C3 = 3.139	C4 = 1.521	C5 = 3.105
R6 = 58.439	R7 = 8.08	R8 = 15.085	R9 = 36.25	Lf = 225.47
L6 = 212.64	L7 = 15.436	L8 = 164.89	L9 = 200.77	Lp = 675.14
C6 = 7.789	C7 = 3.136	C8 = 0.586	C9 = 11.1	D1 = D2 = 0.2

hexagonal patch and a sample of four locations and their effects on the S_{11} is plotted in Figure 5. It is seen that it affects the impedance matching over the complete frequency range and the central location is the closest position to the SWB behavior. After that, the PIN diode is placed inside the slot and the effect of inserting one or two diodes is plotted in Figure 6(a) for the OFF state and Figure 6(b) for the ON state. Inserting two PIN diodes has modified the notch level and the wideband characteristics for the ON state and SWB range in the OFF state as well. Then the distance between the

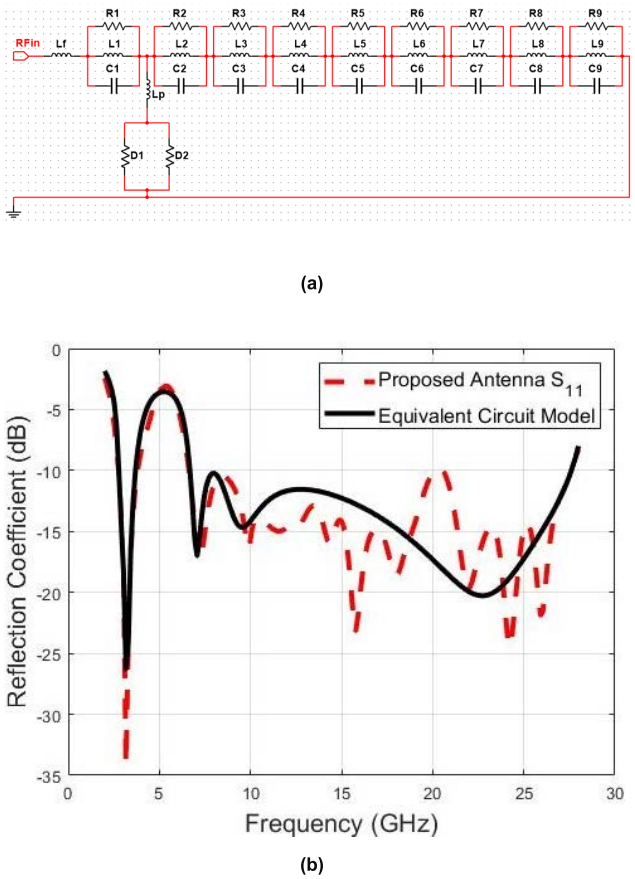

FIGURE 11. (a) Equivalent circuit model and (b) reflection coefficient of the equivalent circuit model when the diodes are in the ON case.

TABLE 3. Values of the components used in the circuit model for the ON case (R (Ω), C (pF), L (pH)).

R1 = 27.948	R2 = 19.705	R3 = 11.053	R4 = 72.466	R5 = 89.642
L1 = 860.54 k	L2 = 394.77	L3 = 2.236 M	L4 = 250.83	L5 = 287.74
C1 = 0.575	C2 = 6.795	C3 = 238.12	C4 = 1.506	C5 = 2.1
R6 = 25.544	R7 = 118.47	R8 = 53.583	R9 = 39.276	Lf = 241.25
L6 = 430.47	L7 = 7.871	L8 = 469.34	L9 = 280.77	Lp = 195.4 k
C6 = 6.4	C7 = 3.964	C8 = 0.149	C9 = 12.114	D1 = D2 = 3

diodes has been monitored and the results are illustrated in Figure 7 where the SWB has been achieved for the OFF-state scenario at 1.25 mm from the patch center.

The antenna surface current density has been studied for the case of both activated diodes to indicate which portion of the antenna is responsible for creating the first resonance and the first notch in the S_{11} curve. As can be seen from Figure 8, the left portion of the slot along with the two diodes

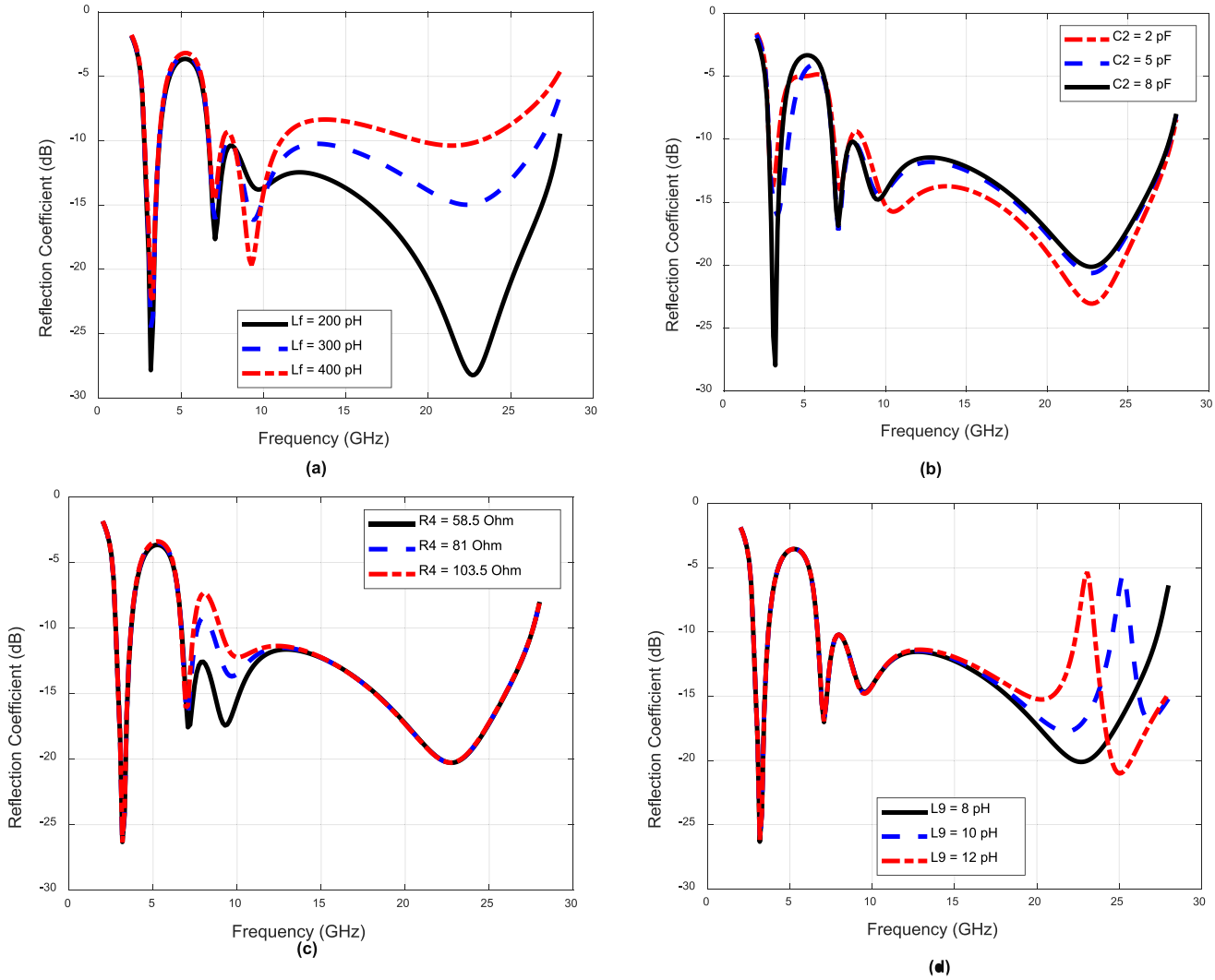

FIGURE 12. Optimization of the circuit components when the diodes are ON for (a) higher frequency band, (b) resonance and notch level, (c) lower frequency band, and (d) higher frequency range.

has a maximum surface current of 50 A/m are responsible for the antenna resonance at 3.175 GHz. Meanwhile, the right slot portion along with the feedline upper terminal has a dominant effect in creating the rejection band at 5.38 GHz.

III. PROPOSED ANTENNA ANALYSIS

A. TIME-DOMAIN CHARACTERISTICS

A substantial aspect of SWB structures is the calculation of the spreading that occurs when the antenna transmits and receives a pulse wave. The pulse based SWB schemes which employ supplying very narrow pulses in time have a rare set of design requests for antennas. As a result, more investigation and assessment into the time domain performance of an SWB antenna are required. The pulse distortion and fidelity factor of the radiated pulse are the most crucial time-domain characteristics. It establishes the amount of pulse distortion caused by the antenna.

In the suggested antenna model, a normalized 5th order Gaussian derivative is set as an input signal. The pulse interval for both ON and OFF states is 190 ps as shown in Figure 9(a) with a little reduction in the input pulse interval for the ON state due to the rejection band, and it will have the SWB spectrum from 2 – 28 GHz in the frequency domain as demonstrated in Figure 9(b). The Nth Gaussian pulse is characterized in the time domain by eq. 2 hence $H_n(t)$ is the nth Hermit polynomial, and its fifth-order polynomial is offered in eq. 3. [35]

$$G(t) = Ae^{-\frac{t^2}{2\sigma^2}} \tag{1}$$

$$G^n(t) = \frac{d^n G}{dt^n} = (-1)^n \frac{1}{(\sqrt{2}\sigma)^2}.H_n\left(\frac{t}{\sqrt{2}\sigma}\right).G(t) \tag{2}$$

$$H_5(t) = 32t^5 - 160t^3 + 120t \tag{3}$$

The Fourier transform of the input signal is plotted in Figure 9(c) which is look like the reflection coefficient for the OFF and ON states produced in the frequency domain and described in Figure 2. The output normalized signal is illustrated in Figure 9(d) for both diodes status, and it has a

TABLE 4. Comparison with different frequency reconfigurable antennas.

Ref. No.	Size		Covered band	Bandwidth GHz (or %)	Notch Gain (dB)	Switching techniques	Rejection band ON/OFF	BDR
	mm^3	$\lambda_o \times \lambda_o$						
[7]	31×45×1.575	0.33×0.23	S, C, X, Ku, K	2.18–44.5(181%)	-	None	-	2389
[8]	36×30×1.6	0.35×0.29	S, C, X, Ku	2.9–14.75(134.3%)	-	None	-	1323.2
[9]	25×30×0.8	0.29×0.35	S, C, X	3.5–33.5(162.2%)	-	None	-	1598
[10]	25×30×0.8	0.25×0.3	S, C, X	3–25.2(157.4%)	-	None	-	2098.7
[11]	25×25×1.6	0.49×0.49	S, C, X	3.71–5.83 (44.4%) 6.05–12.15(67%)	-8	None	-	15.4
[12]	40×70×1.6	0.27×0.47	S, C, X	2–6(100%)	0.9, 5.8, 1.9	None	-	788
[17]	26×36.5×1	0.22×0.31	S, C, X	2.52–9.32 (114.9%)	-4.5	2 PIN diodes 2 varactors	No	1684.8
[18]	50×60×1	0.31×0.37	S, C, X	1.86–10.89 (141.6%)	-9	3 PIN diodes	yes	1234.5
[19]	31×18×0.8	0.32×0.19	S, C, X	3.1 – 12 (117.9%)	- 2.573	2 PIN diodes	yes	1939.1
[20]	60×65×1.6	1.4×1.52	S, C, X, Ku	7–15 (72.7%)	-3.125	4 PIN diodes	No	34.2
[21]	30×30×0.8	0.28×0.28	S, C, X, Ku	2.8–17.9 (145.9%)	-1.33	2 PIN diodes 2 varactors	yes	1861
[22]	8×27.5×1.6	0.07×0.26	S, C, X	2.8–12.6 (127.3%)	-3.55	1 PIN diodes	yes	6994.5
[23]	49.4×35×0.257	0.5×0.35	S, C, X	3–10 (107.7%)	-1.896	2 varactors	No	615.4
[24]	33×21×1.6	0.33×0.21	S, C, X	3–10.6 (111.8%)	-3, -5	2 PIN diodes	yes	1613.3
[25]	24×12×0.787	0.25×0.12	S, C, X	3.1–11(112.1%)	-3, -5	2 PIN diodes	yes	3736.7
[26]	20×20×0.8	0.18×0.18	S, C, X	2.7–10.7 (119.4%)	-3.26, -3.14	2 PIN diodes	yes	3685.2
[27]	30×40×0.76	0.2×0.27	S, C, X	2–8 (120%)	-2, -4	2 varactors	No	2222.2
[28]	40×40×0.16	0.2×0.2	S	1.48–1.99 (29.4%)	-	1 PIN diode	No	735
This work	**36×36×1.6**	**0.4×0.4**	**S, C, X, Ku, K**	**3.37–27.71 (156.6%)**	**-4.34**	**2 PIN diodes**	**yes**	**978.8**

pulse width of fewer than 1.5 ns and less than 1.4 ns for the OFF and ON states respectively, in which the signal distortion is around 60% in the first 0.5 ps, then it reduces rapidly after that.

B. EQUIVALENT CIRCUIT MODEL

The suggested SWB antenna equivalent circuit model has been optimized using the ADS software for both OFF and ON states of the diodes and their calculated S_{11} are plotted and investigated in this section. The equivalent circuit model for SWB antenna in its OFF state is shown in Figure 10(a), it consists of an inductor in series with the first parallel RLC circuit to represent the tapered feedline, then an induct'r 'Lp' in series with two shunt capacitors of 0.2 pF that representing the two diodes in their OFF states. After that eight cascaded RLC circuits produce the SWB behavior [3]. The equivalent circuit S_{11} compared to the HFSS model is depicted in Figure 10(b) for the OFF case where the SWB range is achieved. The detailed optimized circuit components value is summarized in Table 2. Similar analyses were conducted for the antenna while the diodes are active with replacing the two shunt capacitors with two shunt resistors of 3Ω and re-optimizing the circuit components value to create a rejection band within 3.81 – 6.62 GHz. The circuit and its S_{11} response are shown in Figure 11 and the optimized values are listed in Table 3.

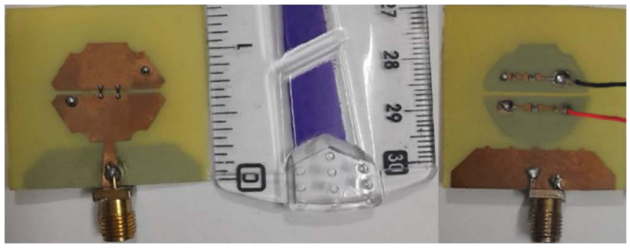

(a)

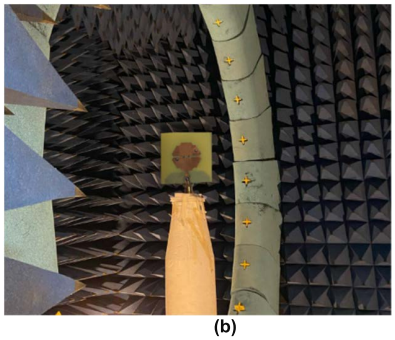

(b)

FIGURE 13. (a) Fabricated prototype (front and back views) and (b) the proposed antenna measurement setup inside the anechoic chamber.

C. PARAMETRIC ANALYSIS OF THE CIRCUIT MODEL

An optimization process has been conducted on all circuit components shown in the Figures above to check their

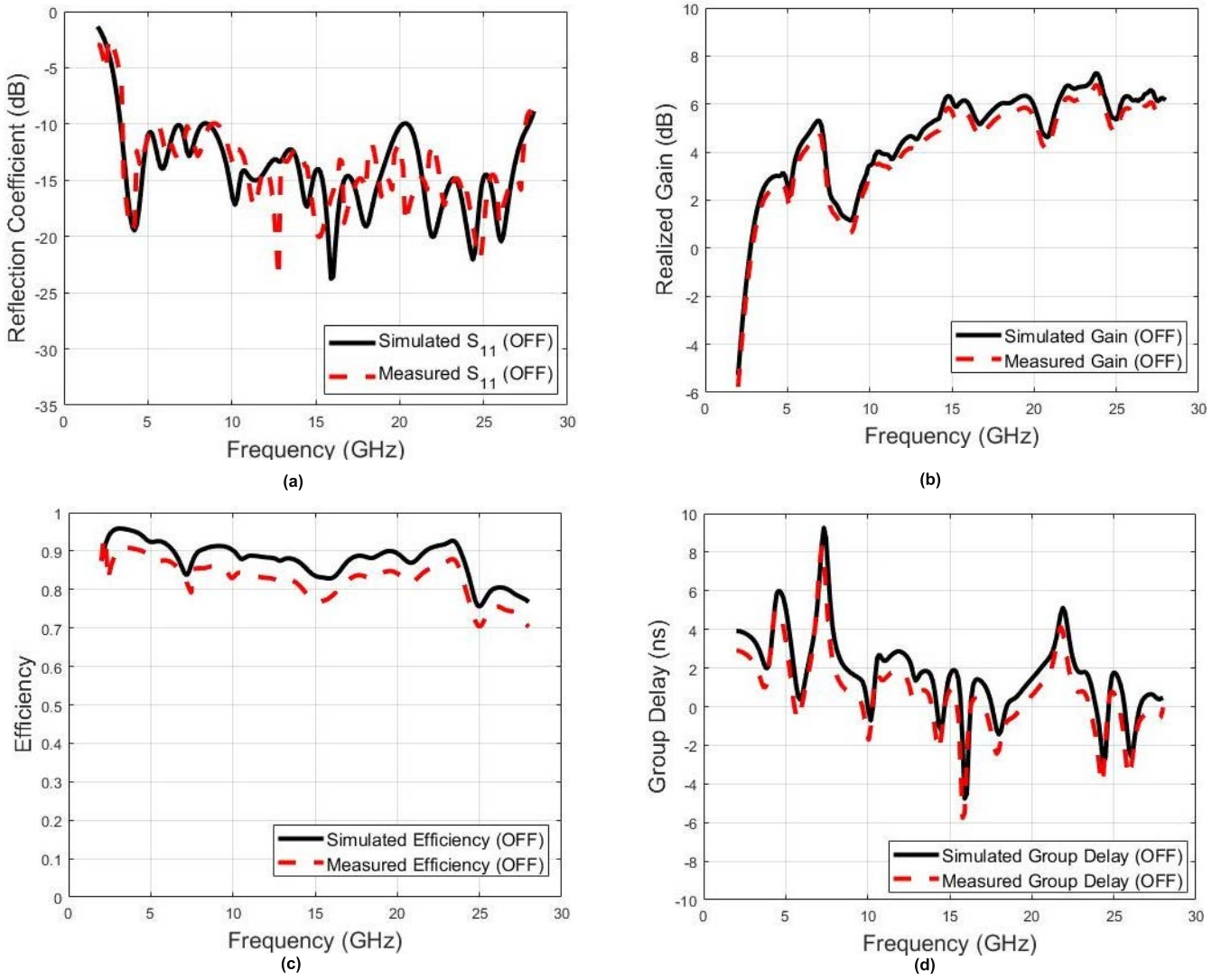

FIGURE 14. The proposed antenna simulated and measured results when the diodes are in the OFF state for (a) Reflection coefficient, (b) Peak realized gain, (c) Radiation efficiency, and (d) Group delay.

impacts on the antenna response and the components with major effects are discussed in this section. Initially, varying the value of the input inductan'e 'Lf' will have an impact on the antenna at higher frequencies (above 10 GHz), the value of t'e 'Lf' for 200 pH, 300 pH, and 400 pH are visualized in Figure 12(a) and as the inductance decreased the S_{11} SWB range will be obtained, and the optimal value is 241.25 pH. The second investigated component 's 'C2' and its effect is shown in Figure 12(b). It has an effect of the rejection band level at 5.38 GHz while maintaining the higher frequency band. The value of resist'r 'R4' is also investigated in Figure 12(c) for its effect on preventing the creation of another notch and hence increasing the frequency range of operation. Finally, the induc'ance 'L9' has a major effect on the antenna S_{11} termination. It is noticed that as the inductance got reduced, the frequency sweep increased to match the desired antenna response as illustrated in Figure 12(d).

IV. FABRICATION AND MEASUREMENTS

The presented antenna has been fabricated on a double-sided FR-4 substrate with a thickness of 1.6 mm and is shown in Figure 13(a), then it is mounted in an anechoic chamber to get its far-field characteristics as shown in Figure 13(b). The measurements are conducted on the antenna S_{11}, peak realized gain, radiation efficiency and group delay as Figures 14 and 15 demonstrate for the OFF and ON cases respectively.

The measured and simulated S_{11} are shown in Figure 14(a) when the diodes are in the OFF state, a good agreement between the results is achieved. The antenna peak realized gain and radiation efficiency measured and simulated curves are shown in Figure 14(b-c) where the maximum gain achieved for the OFF state is 7.28 dB at 23.84 GHz and the minimum value within the operating range is 1.15 dB at 8.89 GHz and for the radiation efficiency it varies between

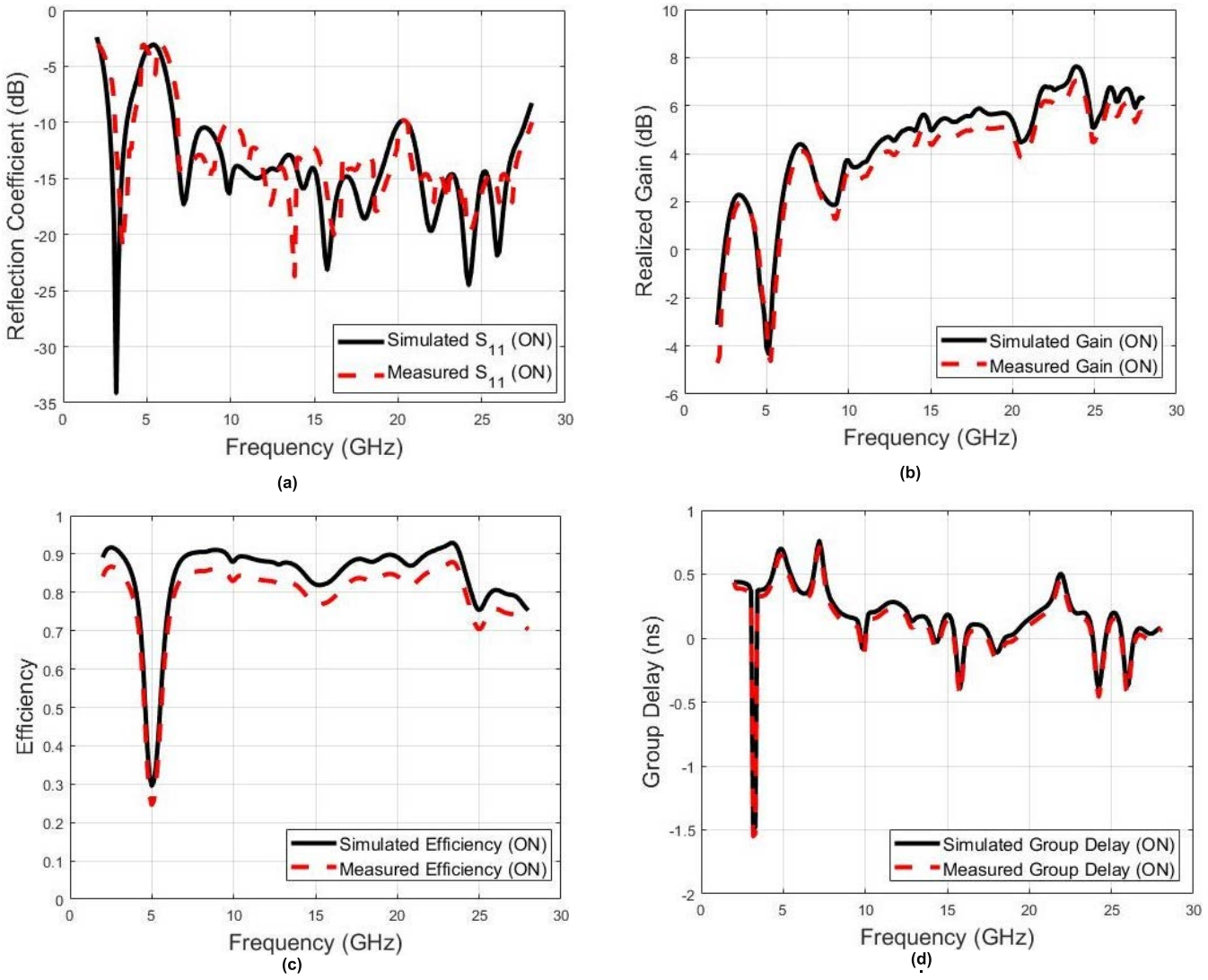

FIGURE 15. The proposed antenna simulated and measured results when the diodes are in the ON state for (a) Reflection coefficient, (b) Peak realized gain, (c) Radiation efficiency, and (d) Group delay.

96 % at 3.37 GHz to 75.6 % at 25 GHz. The group delay in the signal across the tested antenna is under 10 ns as shown in Figure 14(d).

A similar comparison between simulated and measured results is obtained for the proposed antenna in the ON states of the PIN diodes. The results in Figure 15(a-c) for S_{11}, peak realized gain, radiation efficiency, and group delay are in good agreement. The antenna has a rejection band around 5.2 GHz with peak realized gain being varied between -4.34 dB at the notch center frequency to 7.63 dB at 23.84 GHz. The achieved maximum efficiency is 92.9 % at 23.32 GHz and the group delay is less than 1 ns.

The suggested antenna radiation pattern has been measured inside the anechoic chamber to validate the simulated results. Both E-plane (YZ-plane) and H-plane (XZ-plane) are shown in Figure 16 when the diodes are in the reverse biased mode for selected frequencies of 4.21 GHz, 10.19 GHz, 17.99 GHz, and 24.36 GHz where the resonances are located. The patterns show an omnidirectional arrangement (along the E-plane) and a quasi-isotropic arrangement (along H-plane) at the lower frequency band (4.21 GHz) then the omnidirectional behavior starts to deteriorate at higher frequencies. The antenna radiation patterns when the diodes are forward biased are plotted in Figure 17 at the first resonant 3.17 GHz, first notch 5.38 GHz, and two other resonances at higher frequencies 15.7 GHz, and 25.9 GHz. As in the OFF scenario, the antenna exhibits an omnidirectional pattern in the E-plane ($\phi = 90°$) at the lower frequency resonance 3.17 GHz with a quasi-isotropic behavior in the H-plane ($\phi = 0°$). The rejection band (5.38 GHz) has an arbitrary pattern without any noticeable major lobes.

The proposed antenna has been compared to other related works available in the literature in various aspects and the comparison is summarized in Table 4. The BDR is computed

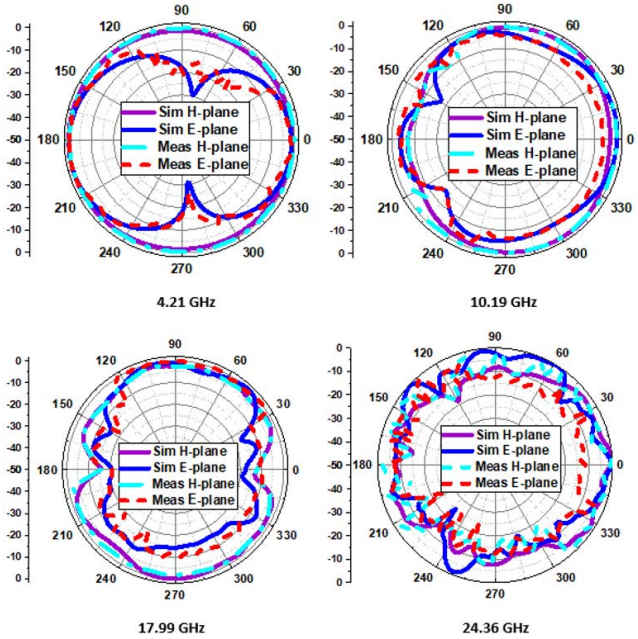

FIGURE 16. The 2D radiation pattern of the antenna in OFF state at 4.21 GHz, 10.19 GHz, 17.99 GHz, and 24.36 GHz.

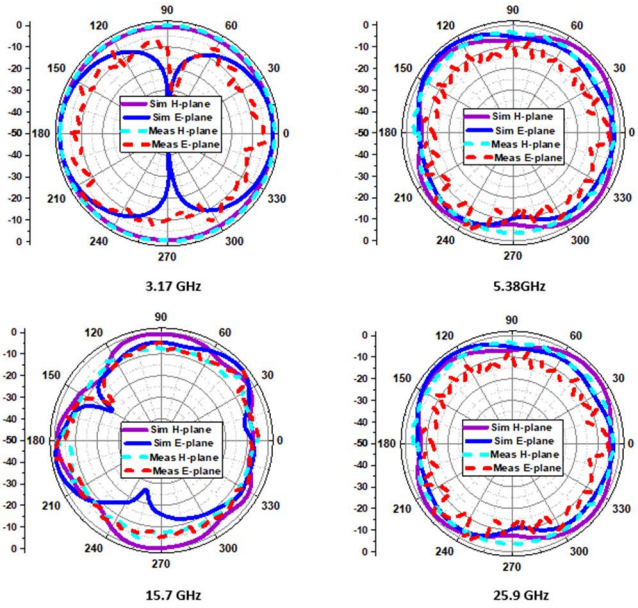

FIGURE 17. The 2D radiation pattern of the antenna in ON state at 3.17 GHz, 5.38 GHz, 15.7 GHz, and 25.9 GHz.

to measure th' antenna's compression which is described as [36]

$$BDR = \frac{\%BW}{\lambda_w x \lambda_L} \tag{4}$$

The proposed work has a smaller antenna size compared to [11], [13], [16] and more bandwidth coverage compared to the listed works. The ON/OFF feature of the rejection band has been done in several works [11], [12], [14], [-], [17]–[19] but by utilizing two PIN diodes and the gain at the notch is quite lower compared to most of the reported works.

V. CONCLUSION

A compact hexagonal frequency diversity antenna with the utilization of two PIN diodes is presented and thoroughly discussed. The antenna patch has been enhanced with a tapered feed and curved edges at its vertices while the partial ground plane is enhanced with beveled edges and five circular sleeves being added to its top edge.

The antenna exhibits an SWB range (3.37 – 27.71) GHz when the diodes are in an OFF state with a rejection band being created at the lower frequency range (3.81 – 6.62) GHz along with two resonances (2.76 – 3.81) GHz and (6.62 – 27.61) GHz when the diodes are in ON state. The antenna achieves a peak gain of 7.28 dB and 7.63 dB at 23.84 GHz with a maximum efficiency of 96 % and 92.9 % for OFF and ON states respectively. The S_{11} at the notch reaches −3.06 dB with a sharp reduction in the gain to reach −4.34 dB at notch center frequency. A time-domain analysis and equivalent circuit models have been introduced and explained for the two diodes scenarios. The conducted measurements confirm the simulated results with a high agreement.

REFERENCES

[1] *Federal Communication Commissions (FCC) (First Report and Order), Revision of Part15 of the Commission's Rules Regarding Ultra-Wideband Transmission Systems*, document ET Docket 98—153, Washington, DC, USA, 2002.

[2] W. Balani, M. Sarvagya, T. Ali, M. Pai M. M., J. Anguera, A. Andujar, and S. Das, "Design techniques of super-wideband Antenna–Existing and future prospective," *IEEE Access*, vol. 7, pp. 141241–141257, 2019.

[3] W. Balani, M. Sarvagya, A. Samasgikar, T. Ali, and P. Kumar, "Design and analysis of super wideband antenna for microwave applications," *Sensors*, vol. 21, no. 2, p. 477, Jan. 2021.

[4] B. Yeboah-Akowuah, E. T. Tchao, M. Ur-Rehman, M. M. Khan, and S. Ahmad, "Study of a printed split-ring monopole for dual-spectrum communications," *Heliyon*, vol. 7, no. 9, Sep. 2021, Art. no. e07928.

[5] T. Okan, "A compact octagonal-ring monopole antenna for super wideband applications," *Microw. Opt. Technol. Lett.*, vol. 62, no. 3, pp. 1237–1244, Mar. 2020.

[6] S. Ahmad, S. Khan, B. Manzoor, M. Soruri, M. Alibakhshikenari, M. Dalarsson, and F. Falcone, "A compact CPW-fed ultra-wideband multi-input-multi-output (MIMO) antenna for wireless communication networks," *IEEE Access*, vol. 10, pp. 25278–25289, 2022, doi: 10.1109/ACCESS.2022.3155762.

[7] M. A. Dorostkar, M. T. Islam, and R. Azim, "Design of a novel super wide band circular-hexagonal fractal antenna," *Prog. Electromagn. Res.*, vol. 139, pp. 229–245, 2013.

[8] R. Kumar, N. Kushwaha, and R. V. S. Ram Krishna, "Design of ultra wideband hexagonal patch slot antenna for high-gain wireless applications," *J. Electromagn. Waves Appl.*, vol. 28, no. 16, pp. 2034–2048, Nov. 2014.

[9] I. Raviteja, C. Padmanjali, D. V. S. Kalyan, B. Alekhya, G. Chakravarthy, and M. V. Ramya, "Analysis and design of hexagonal patch antenna with fractals for wide band applications," *Int. J. Innov. Technol. Exploring Eng. (IJITEE)*, vol. 8, no. 8, pp. 583–587, 2019.

[10] N. K. Darimireddy, R. R. Reddy, and A. M. Prasad, "A miniaturized hexagonal-triangular fractal antenna for wide-band applications [antenna applications corner]," *IEEE Antennas Propag. Mag.*, vol. 60, no. 2, pp. 104–110, Apr. 2018.

[11] R. Boopathi Rani and S. K. Pandey, "A parasitic hexagonal patch antenna surrounded by same shaped slot for WLAN, UWB applications with notch at vanet frequency band," *Microw. Opt. Technol. Lett.*, vol. 58, no. 12, pp. 2996–3000, Dec. 2016.

[12] Chandrabhan and A. Kumar, "Triple band notch loaded hexagonal patch stacked antenna," *Int. J. Eng. Technol. (IJET)*, vol. 9, no. 3, pp. 2485–2490, Jun. 2017.

[13] S. Ahmad, K. N. Paracha, Y. A. Sheikh, A. Ghaffar, A. D. Butt, M. Alibakhshikenari, P. J. Soh, S. Khan, and F. Falcone, "A metasurface-based single-layered compact AMC-backed dual-band antenna for off-body IoT devices," *IEEE Access*, vol. 9, pp. 159598–159615, 2021, doi: 10.1109/ACCESS.2021.3130425.
[14] S. Ahmad, U. Ijaz, S. Naseer, A. Ghaffar, M. A. Qasim, F. Abrar, N. O. Parchin, C. H. See, and R. Abd-Alhameed, "A jug-shaped CPW-fed ultra-wideband printed monopole antenna for wireless communications networks," *Appl. Sci.*, vol. 12, no. 2, p. 821, Jan. 2022.
[15] W. A. Awan, N. Hussain, A. Ghaffar, S. I. Naqvi, A. Zaidi, M. Hussain, and X. J. Li, "A low-profile frequency reconfigurable antenna for mmWave applications," in *WITS* (Lecture Notes in Electrical Engineering), vol. 745, S. Bennani, Y. Lakhrissi, G. Khaissidi, A. Mansouri, and Y. Khamlichi, Eds. Singapore: Springer, 2020.
[16] Y. S. Faouri, S. Ahmad, N. O. Parchin, C. H. See, and R. Abd-Alhameed, "A novel meander bowtie-shaped antenna with multi-resonant and rejection bands for modern 5G communications," *Electronics*, vol. 11, no. 5, p. 821, Mar. 2022.
[17] W. Wu, Y.-B. Li, R.-Y. Wu, C.-B. Shi, and T.-J. Cui, "Band-notched UWB antenna with switchable and tunable performance," *Int. J. Antennas Propag.*, vol. 2016, pp. 1–6, Jun. 2016.
[18] Y. Alnaiemy and L. Nagy, "A novel UWB monopole antenna with reconfigurable band notch characteristics based on PIN diodes," *Infocommunications J.*, vol. 13, no. 3, pp. 33–44, 2021.
[19] L. Han, J. Chen, and W. Zhang, "Compact UWB monopole antenna with reconfigurable band-notch characteristics," *Int. J. Microw. Wireless Technol.*, vol. 12, no. 3, pp. 252–258, Apr. 2020.
[20] T. V. Ramakrishna, B. T. P. Madhav, N. Kiran, B. Sravani, N. Vamsi, and K. L. Yamini, "Frequency reconfigurable antenna for Ku-band applications," *ARPN J. Eng. Appl. Sci.*, vol. 12, no. 22, pp. 6527–6532, 2017.
[21] S. A. Aghdam, "Reconfigurable antenna with a diversity filtering band feature utilizing active devices for communication systems," *IEEE Trans. Antennas Propag.*, vol. 61, no. 10, pp. 5223–5228, Oct. 2013.
[22] A. Toktas and M. Yerlikaya, "A compact reconfigurable ultra-wideband G-shaped printed antenna with band-notched characteristic," *Microw. Opt. Technol. Lett.*, vol. 61, no. 1, pp. 245–250, Jan. 2019.
[23] A. K. Horestani, Z. Shaterian, J. Naqui, F. Martín, and C. Fumeaux, "Reconfigurable and tunable S-shaped split-ring resonators and application in band-notched UWB antennas," *IEEE Trans. Antennas Propag.*, vol. 64, no. 9, pp. 3766–3776, Sep. 2016.
[24] H. Medkour, M. Cheniti, A. Narbudowicz, S. Das, E. Vandelle, and T. P. Vuong, "Coplanar waveguide-based ultra-wide band antenna with switchable filtering of Wimax 3.5 GHz and WLAN 5 GHz signals," *Microw. Opt. Technol. Lett.*, vol. 62, no. 6, pp. 2398–2404, Jun. 2020.
[25] H. Yang, X. Xi, L. Wang, Y. Zhao, X. Shi, and Y. Yuan, "Design of reconfigurable filtering ultra-wideband antenna with switchable band-notched functions," *Int. J. Microw. Wireless Technol.*, vol. 11, no. 4, pp. 368–375, May 2019.
[26] B. Badamchi, J. Nourinia, C. Ghobadi, and A. V. Shahmirzadi, "Design of compact reconfigurable ultra-wideband slot antenna with switchable single/dual band notch functions," *IET Microw., Antennas Propag.*, vol. 8, no. 8, pp. 541–548, Jun. 2014.
[27] H. Ayadi, J. Machac, S. Beldi, and L. Latrach, "Planar hexagonal antenna with dual reconfigurable notched bands for wireless communication devices," *Radioengineering*, vol. 30, no. 1, pp. 25–33, Apr. 2021.
[28] S. S. V., G. Augustin, C. K. Aanandan, P. Mohanan, and K. Vasudevan, "A reconfigurable dual-frequency slot-loaded microstrip antenna controlled by pin diodes," *Microw. Opt. Technol. Lett.*, vol. 44, no. 4, pp. 374–376, 2005.
[29] K. P. Ray and S. Tiwari, "Ultra-wideband printed hexagonal monopole antennas," *IET Microw., Antennas Propag.*, vol. 4, no. 4, pp. 437–445, 2010.
[30] D. M. Pozar, "Rectangular cavity modes," *Microwave Engineering*, vol. 120, 3rd ed. New York, NY, USA: Wiley, 2005.
[31] C.-C. Lin, K.-Y. Kan, and H.-R. Chuang, "A 3-8-GHz broadband planar triangular sleeve monopole antenna for UWB communication," in *Proc. IEEE Antennas Propag. Soc. Int. Symp.*, Jun. 2007, pp. 5741–5744.
[32] M. Abdelazeez and A. Sharif, "Enhanced UWB printed monopole antenna based on ground plane modifications," *Jordanian J. Comput. Inf. Technol. (JJCIT)*, vol. 4, no. 1, pp. 25–33, 2018.
[33] Y. S. Al-Faouri, N. M. Awad, and M. K. Abdelazeez, "Enhanced ultra-wide band hexagonal patch antenna," *Jordanian J. Comput. Inf. Technol.*, vol. 4, no. 3, pp. 150–158, 2018.
[34] *Datasheet for Infineon BAR50-02V, Silicon PIN Diode*. Infineon Technologies AG. Accessed: Apr. 8, 2022. [Online]. Available: http://www.https://www.infineon.com/cms/en/product/rf-wireless-control/rf-diode/rf-pin-diode/antenna-switch/bar50-02v/.
[35] M. Mighani and M. Akbari, "New UWB monopole planer antenna with dual band notched," *Prog. Electromagn. Res. C*, vol. 52, pp. 153–162, 2014.
[36] M. Kumar and V. Nath, "A circularly polarized printed elliptical wide-slot antenna with high bandwidth-dimension-ratio for wireless applications," *Wireless Netw.*, vol. 26, no. 7, pp. 5485–5499, Oct. 2020.

YANAL FAOURI (Senior Member, IEEE) was born in Amman, Jordan, in 1985. He received the B.Sc. degree in electrical engineering from The University of Jordan, Amman, Jordan, in 2007, and the M.Sc. and Ph.D. degrees in electrical engineering from the King Fahd University of Petroleum and Minerals (KFUPM) Dhahran, Saudi Arabia, in 2010 and 2014, respectively. In 2014, he joined the Department of Electrical Engineering, Philadelphia University. Since September 2015, he has been an Assistant Professor at the Department of Electrical Engineering, The University of Jordan. He has published over 30 research papers in peer-reviewed journals and conferences around the world. His research interests include antenna design, applied electromagnetics, RF and microwave circuit design, dielectric-loaded waveguides, printed antennas, compact multiband antennas, and electromagnetic compatibility. He serves as a Reviewer for a number of prestigious journals, including IEEE Access, IEEE Transactions on Components, Packaging and Manufacturing Technology (TCPMT), *International Journal of Applied Electromagnetics and Mechanics* (IJAEM), *International Journal of Communication Systems* (IJCS), and the *Microwave and Optical Technology Letters* (MOTL).

SAROSH AHMAD (Student Member, IEEE) received the bachelor's degree in electrical engineering with specialization in telecommunication from the Department of Electrical Engineering and Technology, Government College University Faisalabad (GCUF), Pakistan, in 2021. He is currently pursuing the master's degree in advanced communication technology with the Department of Signal Theory and Communications, Universidad Carlos III de Madrid (UC3M), Madrid, Spain. He has published 15 conference papers, 30 high indexed international journals, and five book chapters by Springer. His research interests include radio-frequency (RF) circuit design, radiofrequency identification (RFID), signals and systems, wearable and flexible antennas, metamaterial-based antennas, implantable antennas, multi-input-multi-output (MIMO) antennas, mm-wave antennas, 5G antennas, antenna arrays, dielectric resonator antennas (DRAs), photonic antennas, fluidic antennas, antenna for the Internet of Things applications, ultra-wideband (UWB) antennas, wideband antennas, reconfigurable antennas, substrate integrated waveguide (SIW) antennas, circularly polarized antennas, terahertz antennas, rectennas for energy harvesting applications, bandpass filters, half- and full-wave filter antennas, active sensors, and the IoT-based communication devices. He is a member of the IEEE Antennas and Propagation Society (APS). During his graduation, he received the fully funded PEEF Scholarship Award from the Prime Minister of Pakistan and the Silver Medal in his bachelor's program. During his volunteer-ship, he contributed himself as a Branch Treasurer at the IEEE GCUF, Faisalabad Subsection, for two years. After the graduation, he again received the fully funded Erasmus Grant Scholarship for his master's program in Madrid. During his graduation research period, he has participated in four international IEEE conferences over the world, where he has presented ten articles mostly in oral presentations. He has presented his two articles in the International Turkish Conferences where he has got the Best Paper Award, one article in the International Moroccan Conference Proceedings and one articl' in IEEE EuCAP'22. He has served as a Volunteer for the 16th IEEE European Conferences on Antennas and Propagations. He has been selected for the fully funded MITACS Internship Program in the nationally ranked University of Canada called Carleton University where he is working as a Researcher in the field of massive MIMO antennas.

SALMAN NASEER received the B.S. and master's degrees in computer science and the Ph.D. degree (Hons.) in computer and information sciences from the Auckland University of Technology, Auckland, New Zealand. He is currently working as an Assistant Professor with the Department of Information Technology, University of Punjab. He has more than 17 years of teaching and research experience. He has numerous research publications in well-reputed international journals and presented his research work at international conferences at Harvard University, USA, Switzerland, and Singapore. His area of research interests include data communication and networks, internet architecture and protocols, network design and management, network security, wireless networks, and object-oriented programming. He is an Active Member of the Network Security Research Group (NSRG), Auckland University of Technology. He is a member of various IEEE societies like IEEE VTS, IEEE ComCos, IEEE Blockchain, IEEE Young Professionals, IEEE Smart Grids, and IEEE Smart Cities.

KHALID ALHAMMAMI (Member, IEEE) was born in 1998. He received the B.Tech. degree (Hons.) in electrical engineering from The University of Jordan, Amman, Jordan, in 2021. He has authored/coauthored several research articles in refereed international journals and conferences. His research interests include microwave communications, 5G antenna design, planar and conformal microstrip antennas, including array mutual coupling, artificial materials (metamaterials), novel antennas, UWB antennas, slot antennas, and MIMO systems. His research interests include modeling of antenna and RF circuits with HFSS, measurements using vector network analyzer, and MATLAB Simulink.

NOOR AWAD was born in 1978. She received the B.Sc. and M.Sc. degrees in electrical engineering (communication field) from The University of Jordan, Amman, Jordan, in 2001 and 2013, respectively. She has authored/coauthored several research articles in different international journals and conferences. Her research interests include planar microstrip antennas, including UWB antennas, MIMO systems, reconfigurable antennas, and multiband antennas. She has been participating in the review process of the IEEE AP-S International Symposium on Antennas and Propagation, since 2016. She participated in the *International Journal of Electrical Engineering and Informatics* (JEEIT), in 2019, and the *International Journal of RF and Microwave Computer-Aided Engineering*, in 2019 and 2020.

ADNAN GHAFFAR received the B.Sc. degree in computer engineering from BZU Multan, Pakistan, in 2010, and the M.E. degree in circuits and systems from Lanzhou Jiaotong University, Lanzhou, China, in 2015. He is currently pursuing the Ph.D. degree in electrical and electronics engineering with the Auckland University of Technology, Auckland, New Zealand. His research interests include RF circuits, reconfigurable antenna, embedded systems, metasurface antenna, flexible, and wearable antenna design.

MOUSA I. HUSSEIN (Senior Member, IEEE) received the B.Sc. degree in electrical engineering from West Virginia Tech, Montgomery, WV, USA, in 1985, and the M.Sc. and Ph.D. degrees in electrical engineering from the University of Manitoba, Winnipeg, Canada, in 1992 and 1995, respectively. From 1995 to 1997, he was with the Research and Development Group, Integrated Engineering Software Inc., Winnipeg, working on developing EM specialized software based on the boundary element method. In 1997, he joined the Faculty of Engineering, Amman University, Amman, Jordan, as an Assistant Professor. He is currently an Professor with the Department of Electrical Engineering, United Arab Emirates University. He has over 100 publications in international journals and conferences. He has supervised several M.Sc. and Ph.D. students. His current research interests include computational electromagnetics, electromagnetic scattering, antenna analysis and design, metamaterial and applications, and material/bio-material characterization, and sensor design for bio applications.